Bifunctional Gold-Coated Magnetic Silica Spheres

Verónica Salgueiriño-Maceira,*,†,‡ Miguel A. Correa-Duarte,§,|| Michael Farle,⊥ Arturo López-Quintela,† Karl Sieradzki,§ and Rodolfo Diaz‡

Instituto de Investigacións Tecnolóxicas, Universidade de Santiago de Compostela, 15701 Santiago de Compostela, Spain, Departamento de Química-Física, Universidade de Vigo, E-36310 Vigo, Spain, Department of Electrical Engineering and Department of Mechanical and Aerospace Engineering, Arizona State University, Tempe 85281, and Fachbereich Physik, Universtität Duisburg-Essen, D-47048 Duisburg, Germany

Received February 7, 2006. Revised Manuscript Received April 6, 2006

A method for the development of bifunctional magnetic and optically tunable nanoparticles with a structural design involving a magnetic iron oxide core (Fe_3O_4/γ-Fe_2O_3) surrounded by a thick silica shell and further covered with an outer shell of gold is reported. These gold-coated magnetic silica spheres take advantage of the strong resonance absorption they show in the visible and near-infrared (NIR) range and can be controlled by using an external magnetic field, which makes them very promising in biomedical applications.

Introduction

Nanoscience and nanotechnology are envisioned to hold promising applications, including biomedical uses.[1] In this way, practical implications of earlier detection and destruction of cancer cells using nanometer particles have strongly emerged in the recent years.[2] As an example of therapeutic procedures using nanoparticles, hyperthermia is used to raise the temperature of a region of the body affected by malignancy or other growths, with the advantage that it allows heating to be restricted to the tumor area.[3] Thermal therapeutics are relatively simple to perform and have the potential of treating tumors embedded in vital regions where surgical resection is not feasible. Furthermore, it has been demonstrated that macromolecules and small particles (size range <400 nm) will extravasate and accumulate in tumors[4] via a passive mechanism referred to as the enhanced permeability and retention (EPR) effect.[5]

The temperature increase required for hyperthermia can be achieved by using fine iron oxide magnetic particles.[6] The physical principle by which a magnetic material can be heated by the action of an external alternating magnetic field is the loss process that occurs during the reorientation of the magnetization of magnetic materials with low electrical conductivity.[7] Another example is nanoshells composed of a dielectric silica core covered by a thin gold shell, which, depending on the relative dimensions of the core radius and shell thickness, show optical resonances that can be tuned from visible to infrared wavelength,[8] including the NIR region where tissue transmissivity is highest because of low scattering and absorption.[9] Therefore, nanoshells can be designed to strongly absorb NIR light, providing a novel means to mediate photothermal ablation of cancer cells, as demonstrated in a series of in vivo studies.[2a,10] With both cases, magnetic nanoparticles or nanoshells, the heating potential is strongly dependent on the particle size and shape,

* To whom correspondence should be addressed. E-mail: vsalgue@usc.es.
† Universidade de Santiago de Compostela.
‡ Department of Electrical Engineering, Arizona State University.
§ Department of Mechanical and Aerospace Engineering, Arizona State University.
|| Universidade de Vigo.
⊥ Universität Duisburg-Essen.

(1) (a) Brigger, I.; Dubernet, C.; Couvreur, P. *Adv. Drug Delivery Rev.* **2002**, *54*, 631. (b) Tartaj, P.; Morales, M. P.; Veintemillas-Verdaguer, S.; González-Carreño, T.; Serna, C. J. *J. Phys. D.: Appl. Phys.* **2003**, *36*, R182. (c) Stella, B.; Arpicco, S.; Peracchia, M. T.; Desmaele, D.; Hoebeke, J.; Renoir, M.; D'Angelo, J.; Cattel, L.; Couvreur, P. *J. Pharm. Sci.* **2000**, *89*, 1452. (d) Mitra, S.; Gaur, U.; Ghosh, P. C.; Maitra, A. N. *J. Controlled Release* **2001**, *74*, 317. (e) Chapon, C.; Franconi, F.; Lemaire, L.; Marescaux, L.; Legras, P.; Saint-Andre, J. P.; Denizot, B.; Le Jeune, J. J. *Invest. Radiol*. **2003**, *38*, 141.

(2) (a) O'Neal, D. P.; Hirsch, L. R.; Halas, N. J.; Payne, J. D.; West. J. L.; *Cancer Lett*. **2004**, *209*, 171. (b) El-Sayed, I. H.; Huang, X.; El-Sayed, M. A.; *Nano Lett*. **2005**, *5*, 829. (c) Gao, X.; Cui, Y.; Levenson, R. M.; Chung, L. W. K.; Nie, S. *Nat. Biotechnol*. **2004**, *22*, 969. (d) Oyewumi, M. O.; Yokel, R. A.; Jay, M.; Coakley, T.; Mumper, R. J. *J. Controlled Release* **2004**, *95*, 613. (e) Ma, Z.; Wu, J.; Zhou, T.; Chen, Z.; Dong, Y.; Tang, J.; Sui, S.-f.; *New J. Chem*. **2002**, *26*, 1795.

(3) (a) Jordan, A.; Scholz, R.; Wust, P.; Fähling, H.; Felix, R. *J. Magn. Magn. Mater*. **1999**, *201*, 413. (b) Jordan, A.; Scholz, R.; Maier-Hauff, K.; Johannsen, M.; Wust, P.; Nadobny, J.; Schirra, H.; Schmidt, H.; Deger, S.; Loening, S.; Lanksch, W.; Felix, R. *J. Magn. Magn. Mater.* **2001**, *225*, 118.

(4) (a) Kong, G.; Braun, R. D.; Dewhirst, M. W. *Cancer Res*. **2000**, *60*, 4440. (b) Hobbs, S. K.; Monsky, W. L.; Yuan, F.; Roberts, W. G.; Griffith, L.; Torchilin, V. P.; Jain, R. K. *Proc. Natl. Acad. Sci. U.S.A.* **1998**, *95*, 4607.

(5) Maeda, H.; Fang, J.; Inutsuka, T.; Kitamoto, Y. *Int. Immunopharmacol*. **2003**, *3*, 319.

(6) (a) Gilchrist, R. K.; Medal, R.; Shorey, W. D.; Hanselman, R. C.; Parrot, J. C.; Taylor, C. B. *Ann. Surg*. **1957**, *146*, 596. (b) Huber, D. L. *Small* **2005**, *1*, 482. (c) Zhang, Y.; Zhang, J. *J. Colloid Interface Sci*. **2005**, *283*, 352. (d) Mornet, S.; Vasseur, S.; Grasset, F.; Duguet, E. *J. Mater. Chem*. **2004**, *14*, 2161. (e) Gupta, A. K.; Gupta, M. *Biomaterials* **2005**, *26*, 3995. (f) Ito, A.; Kuga, Y.; Honda, H.; Kikkawa, H.; Horiuchi, A.; Watanabe, Y.; Kobayashi, T. *Cancer Lett*. **2004**, *212*, 167.

(7) (a) Hiergeist, R.; Andrä, W.; Buske, N.; Hergt, R.; Hilger, I.; Richter, U.; Kaiser, W. *J. Magn. Magn. Mater*. **1999**, *201*, 420.

(8) Oldenburg, S. J.; Jackson, J. B.; Westcott, S. L.; Halas, N. J. *Appl. Phys. Lett*. **1999**, *75*, 2897.

(9) Weissleder, R. *Nat. Biotechnol*. **2001**, *19*, 316.

(10) Hirsch, L. R.; Stafford, R. J.; Bankson, J. A.; Sershen, S. R.; Rivera, B.; Price, R. E.; Hazle, J. D.; Halas, N. J.; West, J. L. *Proc. Natl. Acad. Sci. U.S.A.* **2003**, *100*, 13549.

10.1021/cm0603001 CCC: $33.50
Published on Web 05/09/2006

and thus having well-defined synthetic routes that are able to produce uniform particles is essential for a rigorous temperature control.

The advantage of the nanoshells compared to the iron oxide nanoparticles is the possibility of engineering them with optical properties suitable for combined imaging and therapy,[11] as they can simultaneously provide both scattering and absorption properties at specific frequencies. On the other hand, the advantage of magnetic nanoparticles is that their movement can be controlled with an external magnetic field so that they can be immobilized close to the targeted tissue.[3b] Composite materials that have both optical properties of gold and magnetic properties of superparamagnetic nanoparticles have already been reported.[12] Herein, we demonstrated the synthesis of bifunctional nanoparticles with both magnetic and optical properties, engineered to simultaneously provide promising possibilities for external control of movement using a magnetic field to direct the particles to cancer tumors and strong absorption of NIR light to provide imaging and photothermal ablation. In this case, however, both functionalities are separated by a thick silica shell in such a way that interactions between both components are avoided.

Experimental Section

$Fe_3O_4/\gamma-Fe_2O_3$ Nanoparticles. Aqueous dispersions of magnetite nanoparticles that were partially oxidized to maghemite were prepared according to Massart's method,[13] on the basis of the coprecipitation of ferrous and ferric ion solutions (1:2 molar ratio). Aqueous $FeCl_3$ (1 M, 20 mL) and 5 mL of $FeSO_4$ (2 M) in HCl (2 M) were added to 250 mL of NH_4OH (0.7 M) under rapid mechanical stirring. Stirring was allowed to continue for 30 min, and the black solid product was then allowed to precipitate. The sediment was redispersed in 50 mL of distilled water, and subsequently three aliquots of 10 mL tetramethylammonium hydroxide solution (1 M) were added, again with rapid stirring. Finally, water was added to the dispersion up to a total volume of 250 mL. The magnetite nanoparticle dispersion was further washed as follows: 4 mL of magnetic nanoparticle solution was dispersed in 50 mL of distilled water, centrifuged, and redispersed in pure water (100 mL).

Silica-Coated Magnetite/Maghemite Particles ($Fe_3O_4/\gamma-Fe_2O_3@SiO_2$). To a mixture of 4.85 mL of NH_4OH (28%), 28.8 mL of H_2O, 27.5 mL of EtOH, and 6.22 mL of the previously washed magnetic nanoparticles in water solution was added an ethanolic solution of TEOS (tetraethyl orthosilicate; 2 mL of TEOS in 30 mL of EtOH) while the solution was mechanically stirred. After mixing, the final volume was 100 mL and the concentration of TEOS, NH_4OH, and H_2O were, respectively, 0.25, 0.35, and 21.4 M. The hydrolysis and condensation of TEOS onto the magnetic nanoparticles was completed in 4 h. The formed particles were centrifuged to eliminate excess reactants and redispersed in 50 mL of pure water.

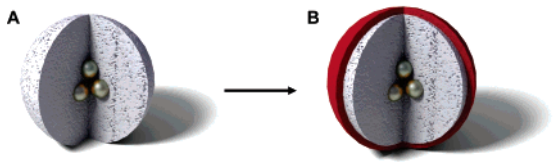

Figure 1. Schematic illustration of magnetic silica spheres coated with an outer shell of gold.

Gold Nanoparticles. Citrate-stabilized 15 nm Au nanoparticles were prepared according to the standard sodium citrate reduction method[14] by adding 5 mL of sodium citrate solution (1 wt %) to 100 mL of an aqueous solution containing $HAuCl_4$ (5×10^{-4} M) while it was boiled and vigorously stirred.

Gold-Coated Magnetic Silica Spheres. A precursor polyelectrolyte film was deposited by the alternate adsorption of PDADMAC (poly(diallyldimethylammonium chloride)), PSS (poly(sodium 4-styrenesulfonate)), and PDADMAC onto the magnetically patterned silica spheres, as indicated elsewhere,[15] in such a way that the polymer selected has an opposite charge to that on the silica spheres; hence, the polymer is predominantly adsorbed through electrostatic interactions. These three layers of polyelectrolytes produce a smoother, more uniform, and positively charged surface onto the magnetic silica spheres. PE_3-coated magnetic silica spheres (NaCl 0.2 M, 1 mL) were mixed with 1 mL of the gold nanoparticle solution, and an adsorption time of 20 min was allowed. The excess of gold seeds was removed by three repeated centrifugation/wash cycles, and the particles were redispersed in 2 mL of pure water.

Gold-Shell Formation. A solid shell of gold was formed onto the magnetic silica spheres step by step by reducing aliquots of $HAuCl_4$ (10 μL, 5×10^{-4} M) with ascorbic acid (10 μL, 0.34×10^{-3} M) in aqueous solution, using the deposited 15 nm Au particles as seeds to template the growth of the shell.

Characterization Methods. TEM images were collected using a Tecnai F20 electron microscope operating at 200 kV. Samples were deposited onto 200 mesh carbon-coated copper grids. Magnetic measurements were carried out using a superconducting quantum interference device (SQUID) magnetometer with fields up to 4 T. UV−vis spectra were collected using a Shimadzu UV-3101PC UV−visible spectrometer over the range 200−1100 nm. All samples were loaded into a quartz cell for analysis.

Results and Discussion

Figure 1 shows a schematic illustration of core−shell nanoparticles with both magnetic and optical functionalities. Silica-coated magnetic nanoparticles (magnetic silica spheres; Figure 1a), further coated with an outer shell of gold (Figure 1b), can be prepared by surrounding iron oxide nanoparticles with a thick silica shell. Once the magnetic silica spheres are accomplished, they can be functionalized with polyelectrolytes in order to increase, smooth, and reverse their negatively charged surface, therefore facilitating the deposition of citrate-stabilized 15 nm gold particles. This deposition

(11) Loo, C.; Lowery, A.; Halas, N.; West, J.; Drezek, R. *Nano Lett.* **2005**, *5*, 709.
(12) (a) Caruntu, D.; Cushing, B. L.; Caruntu, G.; O'Connor, C. J. *Chem. Mater.* **2005**, *17*, 3398. (b) Ban, Z.; Barnakov, Y. A.; Li, F.; Golub, V. O.; O'Connor, C. J. *J. Mater. Chem.* **2005**, *15*, 4660, (c) Cushing, B. L.; Golub, V. O.; Henry, M.; Oliva, B. L.; Cook, E.; Holmes, C. W.; O'Connor, C. J. *Nanotechnology* **2005**, *16*, 1701. (d) Wang, L.; Luo, J.; Fan, Q.; Suzuki, M.; Suzuki, I. S.; Engelhard, M. H.; Lin, Y.; Kim, N.; Wang, J. Q.; Zhong, C.-J. *J. Phys. Chem. B* **2005**, *109*, 21593. (e) Stoeva, S. I.; Huo, F.; Lee, J.-S.; Mirkin, C. A. *J. Am. Chem. Soc.* **2005**, *127*, 15362. (f) Spasova, M.; Salgueiriño-Maceira, V.; Schlachter, A.; Hilgendorff, M.; Giersig, M.; Liz-Marzán, L. M.; Farle, M. *J. Mater. Chem.* **2005**, *15*, 2095.
(13) Massart, R. *IEEE Trans. Magn.* **1981**, *MAG-17*, 1247.
(14) Enüstün, B. V.; Turkevich, J. *J. Am. Chem. Soc.* **1963**, *85*, 3317.
(15) (a) Caruso, F.; Lichtenfeld, H.; Giersig, M.; Möhwald, H. *J. Am. Chem. Soc.* **1998**, *120*, 8523. (b) Caruso, F.; Caruso, R. A.; Möhwald, H. *Science* **1998**, *282*, 1111. (c) Caruso, F.; Caruso, R. A.; Möhwald, H. *Chem. Mater.* **1999**, *11*, 3309. (d) Caruso, F.; *Chem.—Eur. J.* **2000**, *6*, 413.

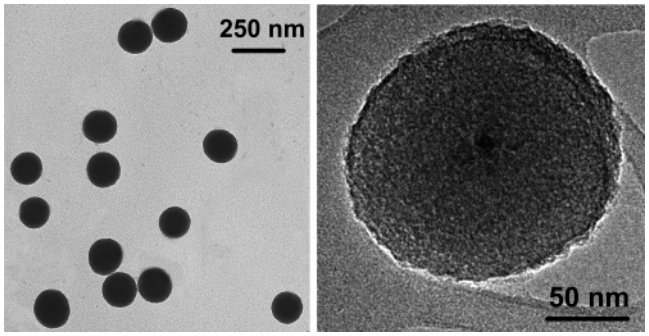

Figure 2. TEM images of silica-coated magnetite/maghemite nanoparticles forming magnetic silica spheres.

creates an outer nanoparticulate shell of gold that shows a plasmon band resonance shifted to higher wavelengths, which is attributable to the coupling between neighboring particles.[16] This nanoparticulate shell becomes a compact shell by reducing more gold onto the seeds, filling the voids between the 15 nm gold particles deposited onto the magnetic silica spheres. At the same time, the more compact the shell, the bigger the red-shift of the absorption band, reaching the NIR range.

The first step was carried out by using magnetite/maghemite nanoparticles (8−10 nm average diameter, see Supporting Information, Figure S1), which were coated with a silica shell using a sol−gel process based on the hydrolysis of TEOS. This step relies on the well-known Stöber method,[17] forming uniform core−shell units. The iron oxide surface has a strong affinity for silica, so no primer was required to promote the deposition and adhesion of silica.[18] Figure 2 shows TEM images of monodisperse and spherical silica-coated iron oxide nanoparticles (170 nm, average diameter). In most of the cases, the magnetic core is composed of more than one iron oxide nanoparticle (see image on the right, Figure 2), because of the aggregation of iron oxide nanoparticles prior to or during the coating process. This fact becomes an advantage when manipulating these core−shell spheres with an external magnetic field, as discussed below. The iron oxide nanoparticles act as seeds for the deposition of the silica shell. By this stepwise seeded Stöber growth process, we grew spherical magnetic silica spheres with a radius of 85 nm; their polydispersity decreased with every growth step, as previously reported for silica particles.[19] Functionalization of these particles with polyelectrolytes and the centrifugation/redispersion cycles did not influence their size and polydispersity. The resulting particles were stable and used in all subsequent steps.

These core−shell structured magnetic silica spheres were characterized by using a superconducting quantum interference device (SQUID) (Figure 3). Figure 3a shows the hysteresis loops measured at 5 and 300 K of silica-coated iron oxide nanoparticles. These magnetic silica spheres are superparamagnetic at room-temperature, reaching a 1.34 emu/g saturation moment. This low saturation magnetization value, far from the saturation magnetization of the magnetite/maghemite nanoparticles used for the preparation of these core−shell magnetic silica spheres ((54 emu/g) (see the Supporting Information, Figure S1), and from reported values (74 emu/g for bulk γ-Fe_2O_3[20] and 5 emu/g for very small γ-Fe_2O_3 particles[21]), can be explained by taking into account the diamagnetic contribution of the thick silica shell surrounding the magnetic cores; the magnetic core corresponds to only 2 wt % of the magnetic silica sphere (calculated taking into consideration the average volumes of the magnetic core and the silica shell). At 5 K, the spheres exhibited ferromagnetic characteristics, including coercivity (H_c = 175 Oe) and remanence. The temperature dependence of the zero-field-cooled/field-cooled (ZFC/FC) magnetization is shown in Figure 3b. Both curves coincide at high temperature and begin to separate as the temperature decreases, showing a maximum (in the case of ZFC) at 120 K. Such behavior is characteristic of superparamagnetism[22] and is due to a progressive deblocking of particles as the temperature increases. It is generally assumed that the temperature of the maximum depends on the average particle size, whereas the temperature at which the FC and ZFC curves start to separate corresponds to the blocking temperature of the largest particles. The difference between both temperatures (T_{max} = 120 K, T_B = 150 K) therefore represents a qualitative measure of the magnetic core size distribution in the silica spheres, which are formed by different numbers of magnetic iron oxide nanoparticles. These magnetic characteristics allow the manipulation of the composite particles, as discussed below.

The formation of the outer shell of gold onto the magnetic silica spheres was examined by transmission electron microscopy (TEM). Figure 4 shows TEM micrographs of bifunctionalized spheres with 15 nm gold seeds deposited onto the surface of the magnetic silica spheres (images on the left) and with an outer gold shell approximately 30 nm thick (images on the right). The formation of the shell of gold was accomplished by combining molecular self-assembly (layer-by-layer (LbL) self-assembly technique[15]) and colloidal growth chemistry (reducing the salt of gold ($HAuCl_4$) using ascorbic acid) following a two-step process to produce particles with an outer shell of gold that is 30 nm thick. The first step for the formation of the outer shell of gold onto the magnetic silica spheres consisted of the deposition of three layers of oppositely charged polyelectrolytes. This method, known as the LbL self-assembly technique, allows for the construction of composite multilayer assemblies. Caruso and co-workers[15] applied this LbL self-assembly technique to coat spherical colloids, on the basis of the previous work of Kotov[23] and Decher[24] that exploited

(16) (a) Caruso, F.; Spasova, M.; Salgueiriño-Maceira, V.; Liz-Marzán, L. M. *Adv. Mater*. **2001**, *13*, 1090. (b) Salgueiriño-Maceira, V.; Caruso, F.; Liz-Marzán, L. M. *J. Phys. Chem. B* **2003**, *107*, 10990.
(17) Stöber, W.; Fink, A.; Bohn, E. *J. Colloid Interface Sci.* **1968**, *26*, 62.
(18) (a) Lu, Y.; Yin, Y.; Mayers, B. T.; Xia, Y. *Nano Lett.* **2002**, *2*, 183. (b) Deng, Y.-H.; Wang, C.-C.; Hu, J.-H.; Yang, W.-L.; Fu, S.-K. *Colloids Surf., A* **2005**, *262*, 87.
(19) Van Blaaderen, A.; van Geest, J.; Vrij, A. *J. Colloid Interface Sci*. **1992**, *154*, 481.
(20) Berkowitz, A. E.; Schuele, W. J.; Flanders, P. J. *J. Appl. Phys*. **1968**, *39*, 1261.
(21) Martínez, B.; Obradors, X.; Balcells, L.; Rouanet, A.; Monty, C. *Phys. Rev. Lett*. **1998**, *80*, 181.
(22) (a) Morrish, A. H. *The Physical Principles of Magnetism*; Wiley: New York, 1965. (b) Morup, S.; Bodker, F.; Hendriksen, P. V.; Linderoth, S. *Phys. Rev. B* **1995**, *52*, 287.
(23) Kotov, N. A.; Dekany, I.; Fendler, J. H. *J. Phys. Chem*. **1995**, *99*, 13065.

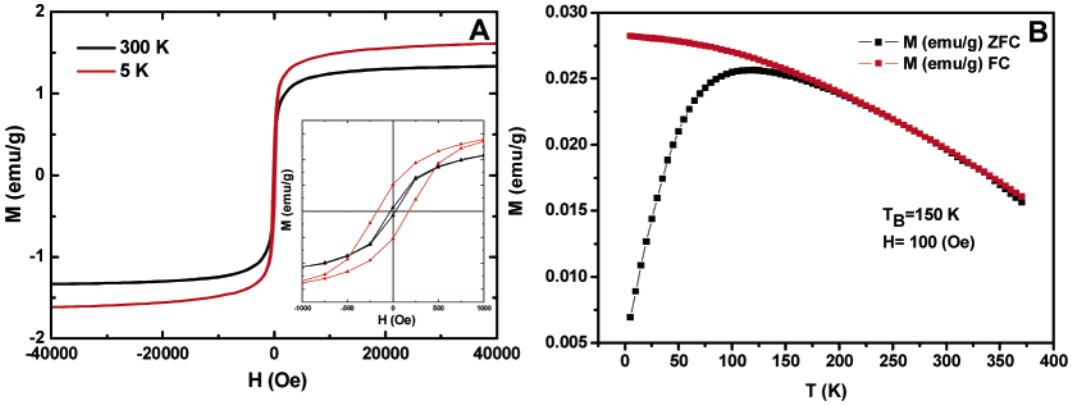

Figure 3. (a) Hysteresis loops recorded at 5 (red line) and 300 K (black line) (inset shows loops at lower magnetic fields) and (b) ZFC/FC curves of magnetic silica spheres.

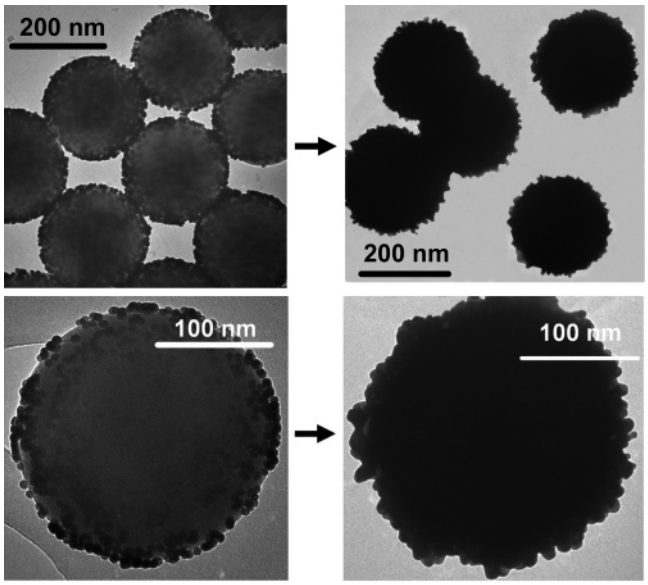

Figure 4. TEM images of the gold shells (right) formed on the magnetic silica spheres by filling the voids between the 15 nm gold particles deposited onto the surface of the magnetic silica spheres (left).

the electrostatic attractions between the charged species to be deposited. The precursor polyelectrolyte film was deposited by the alternate adsorption of PDADMAC (poly(diallyldimethylammonium chloride)), PSS (poly(sodium 4-styrenesulfonate)), and PDADMAC onto magnetically primed silica spheres. These three layers of polyelectrolytes produce a smoother, more uniform, and positively charged surface onto the magnetic silica spheres. After the deposition of three layers of polyelectrolytes and again exploiting the electrostatic attraction between the positively charged surface of the magnetic silica spheres (due to the outer layer of polyelectrolyte, PDADMAC) and the negatively charged surface of the citrate-stabilized 15 nm gold nanoparticles, we infiltrated gold seeds into the pre-assembled polyelectrolyte multilayers[25] and deposited them onto the magnetic silica spheres, as shown in the images on the left in Figure 4. This deposition of gold particles results in an increase in the particle diameter from 170 to 206 nm, in close agreement with the diameter of the Au nanoparticles (~15 nm) and the thickness of the polyelectrolyte film (~3 nm), indicating that approximately a single monolayer of nanoparticles is deposited.

The strong optical extinction of Au nanoparticles is due to a collective oscillation of the free electrons known as the plasmon resonance (see the Supporting Information, Figure S2).[26] In addition to the dielectric functions of the metal and the embedding medium, the optical resonance is also a function of the size and the shape of the gold particle. Although the tunability of the resonance of pure metal particles is relatively limited, gold in the form of aggregates,[27] platelets,[28] and rods[29] can shift the peak plasmon resonance wavelength hundreds of nanometers away into the near-infrared range.[26a,30] The aqueous solution of gold nanoparticles (15 nm) used for the deposition onto the surface of the magnetic silica spheres has a peak absorption wavelength at 518 nm (Figure 5, inset, and Supporting Information, Figure S2). At the initial stage of the shell formation, when the Au nanoparticles are deposited onto the spherical substrates, the spectrum red-shifts to ~540 nm (Figure 5, spectrum 2) because of strong interparticle interactions and the coupling of the surface plasmons of neighboring particles,[16] indicating that the deposited gold nanoparticles behave as discrete but coupled particles. The 15 nm gold colloids attached to the surface of the magnetic silica spheres were used to template the growth of the solid gold shell. To prevent the growth of pure gold particles in the formation of the gold shell in the next reaction step, we removed all non-attached gold nanoparticles from the dispersion of the gold-coated magnetic silica spheres by several centrifugation/redispersion cycles.

A method for the formation of gold shells by the reductive growth of small gold nanoclusters on silica spheres has

(24) (a) Decher, G. *Science* **1997**, *277*, 1232. (b) Decher, G.; Hong, J.-D. *Makromol. Chem., Macromol. Symp.* **1991**, *46*, 321.
(25) (a) Liang, Z.; Susha, A.; Caruso, F. *Chem. Mater.* **2003**, *15*, 3176. (b) Radt, B.; Trevor, T. A.; Caruso, F. *Adv. Mater.* **2004**, *16*, 2184.
(26) (a) Hache, F.; Richard, D.; Flytzanis, C.; Kreibig, U. *Appl. Phys. A: Solids Surf.* **1988**, *47*, 347. (b) Perner, M.; Bost, P.; Lemmer, U.; von Plessem, G.; Feldmann, J.; Becker, U.; Menig, M.; Schmitt, M.; Schmidt, H. *Phys. Rev. Lett.* **1997**, *78*, 2192.
(27) (a) Turkevich, J. *Gold Bull.* **1985**, *18*, 86. (b) Quinten, M.; Kreibig, U.; *Surf. Sci.* **1986**, *172*, 557.
(28) Weisner, J.; Wokaun, A. *Chem. Phys. Lett.* **1989**, *157*, 569.
(29) (a) Pérez-Juste, J.; Liz-Marzán, L. M.; Carnie, S.; Chan, D. Y. C.; Mulvaney, P. *Adv. Func. Mater.* **2004**, *14*, 571. (b) Jana, N. R.; Gearheart, L.; Murphy, C. J. *Adv. Mater.* **2001**, *13*, 1389.
(30) Kreibig, U.; Vollmer, M. *Optical Properties of Metal Clusters*; Springer: New York, 1995.

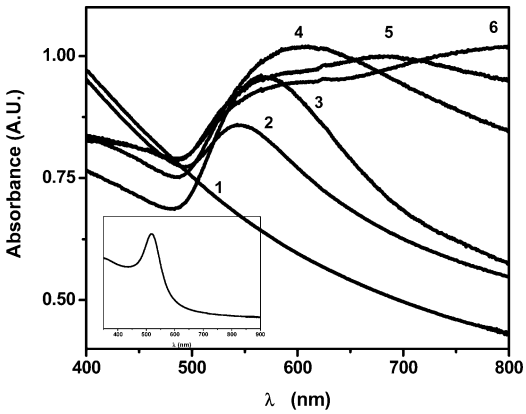

Figure 5. UV−vis spectra illustrating the formation of the gold shell on the magnetic silica spheres, showing the red-shift of the absorption band to the NIR. Spectra numbered as 1 and 2 correspond to the magnetic silica spheres before and after deposition of the 15 nm gold nanoparticles. Spectra numbered 3−6 illustrate the filling of the voids between the 15 nm gold nanoparticles until the formation of the compact gold shell. Inset, absorption spectrum of the 15 nm Au nanoparticles (seeds) in aqueous solution.

already been developed by Oldenburg[31] and Graf,[32] although the principal goal in that case was to grow the gold nanoparticles in a simpler way while having the ability to remove the new gold particles that nucleate in solution. Figure 4 (TEM images on the right) shows gold nanoshells produced using the 15 nm gold seeds. These bifunctionalized gold-coated magnetic silica spheres consist of a 170 nm core (silica-coated magnetite/maghemite nanoparticles) encased by an outer gold layer approximately 30 nm thick. The thickness of the gold shells was calculated by subtracting the magnetic silica sphere diameter obtained by TEM measurements. This method, comprising an initial nanoparticulate gold shell, has the advantage of simplifying the process for completing the formation of the solid shell when compared to that previously reported,[31] because gold (from the reduction of $HAuCl_4$ using ascorbic acid) only has to fill the voids between the nanoparticles in the second step. As a result, the gold nanoparticles distributed over the surface of the magnetic silica spheres were growing at the same time, reaching a shell of 30 nm thickness, although they were fairly rough, as shown in the TEM images (Figure 4, right). This roughness can be explained by taking into account that the reduced gold not only fills the voids between the nanoparticles but also grows on the particles themselves. These gold-coated magnetic silica spheres are stable in water, but at this point, continuing to increase the shell thickness just by adding more gold salt results in lower colloidal stability and aggregation of the core−shell particles.

Figure 5 shows the evolution of the optical absorption of the nanocomposites as the formation of the outer gold shell onto the magnetic silica spheres progresses. Spectrum 1 corresponds to original magnetic silica spheres, whereas number 2 corresponds to the same magnetic silica spheres after the deposition of one monolayer of 15 nm gold nanoparticles. The subsequent filling of the voids (reducing the gold salt $HAuCl_4$ using ascorbic acid) between the gold nanoparticles onto the magnetic silica spheres leading to the formation of a compact gold shell can be followed by the red-shifting of the maxima of the spectra (Figure 5, spectra 3−6). Once the seeds coalesce, the peaks in the spectra become distorted into a broad band, indicating gold particles with a distribution of different sizes and an increase in thickness of the metal coating.[25,31b] Once the shell is complete (30 nm thick, determined by TEM), the peak absorbance reaches the NIR range, in close agreement with theoretical calculations.[33] Particles with an incomplete gold shell (spectra 4 and 5) show a completely different spectrum than those with a closed gold shell (spectrum 6). Whereas for particles with smaller cores, the extinction spectrum is mainly determined by dipole and quadrupole contributions and shows only a single strong peak at 680 nm,[32] the spectra of particles with bigger cores, as in this case, have additional contributions of higher-order resonances and are therefore more complicated functions with a broader band of several maxima.[32]

Halas and co-workers reported that by varying the core and shell thicknesses, they can place the optical resonance virtually anywhere across the visible or infrared regions of the optical spectrum. These composite gold-coated magnetic silica spheres with a 170 nm average diameter of the core and a gold shell 30 nm thick presents a core diameter:shell thickness ratio of 5.6, therefore offering an optical resonance wavelength around 800 nm, as previously calculated.[31] The optical properties of composite spheres (dielectric silica core and metallic gold shell) have been explained by means of a plasmon hybridization model, where the plasmon resonance is a sensitive function of the inner and outer radius of the shell layer.[33] These calculations, performed on the basis of the silica core-gold shell systems, also fit for these systems of gold-coated magnetic silica spheres, because the iron oxide inner core is relatively small compared to the whole magnetic silica sphere, therefore slightly varying the dielectric constant.

It is generally assumed that the surface features are more important than those of the core, because the surface would be in direct contact with the blood and organs in biomedical applications.[34] Taking this into account, researchers have already functionalized gold nanoshells with self-assembled molecules that facilitate nanoshell purification and offer new strategies for nanoshell manipulation and applications,[35] ensuring the possibility of applications in biological environments. Although nanoshells are composed of elements generally understood to be biocompatible, their surfaces have also been grafted using simple molecular self-assembly techniques to further improve biocompatibility.[35,36]

On the other hand, the multiple magnetic core of the nanocomposites permits us to direct them to specific locations when they are manipulated by an external magnetic field. This can be monitored through the photographs in Figure 6,

(31) (a) Oldenburg, S. J.; Averitt, R. D.; Westcott, S. L.; Halas, N. J. *Chem. Phys. Lett.* **1998**, *288*, 243. (b) Oldenburg, S. J.; Westcott, S. L.; Averitt, R. D.; Halas, N. J. *J. Chem. Phys.* **1999**, *111*, 4729.
(32) Graf, C.; van Blaaderen, A. *Langmuir* **2002**, *18*, 524.
(33) (a) Radloff, C.; Halas, N. J. *Nano Lett.* **2004**, *4*, 1323. (b) Prodan, E.; Radloff, C.; Halas, N. J.; Nordlander, P. *Science* **2003**, *302*, 419.
(34) Choi, S.-W.; Kim, W.-S.; Kim, J.-H. *J. Dispersion Sci. Technol.* **2003**, *24*, 475.
(35) Pham, T.; Jackson, J. B.; Halas, N. J.; Lee, T. R. *Langmuir* **2002**, *18*, 4915.
(36) Hirsch, L. R.; Jackson, J. B.; Lee, A.; Halas, N. J.; West, J. L. *Anal. Chem.* **2003**, *75*, 2377.

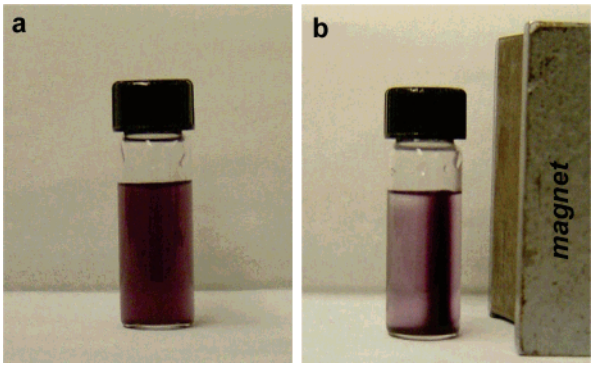

Figure 6. Photograph of a solution of gold-coated magnetic silica spheres in the (a) absence or (b) presence of a magnetic field gradient.

which illustrates their magnetic nature. In the absence of a magnet, the dispersion of magnetic and optically active particles is dark red-violet (left). When an external magnetic field is applied, the nanocomposites concentrate along the magnet, rendering the dispersion transparent, as shown in the photograph on the right, and can be redispersed again when the magnet is removed.

Conclusion

In summary, by exploiting molecular self-assembly (layer-by-layer (LbL) self-assembly technique) and colloidal growth chemistry, we can coat magnetic silica spheres with an outer shell of gold, functionalizing the nanocomposite core−shell spheres with optical and magnetic properties. These particles not only possess a highly tunable plasmon resonance in the visible−near-infrared range but also can be manipulated using an external magnetic field; this makes them very promising in fields concerning the selective destruction of targeted carcinoma cells through photothermal therapy, because they can be controlled through the blood stream using an external magnetic field, therefore favoring their selective accumulation at the targeted pathologic tissue.

Acknowledgment. The authors acknowledge the Center of Solid State Science (Arizona State University) for TEM access and Dr. M. Spasova (University of Duisburg-Essen) for the help with magnetic measurements. V. S.-M. and M.A.C.-D. acknowledge financial support from the Isidro Parga Pondal Program (Xunta de Galicia, Spain).

Supporting Information Available: Figures showing hysteresis loops at 5 and 300 K and TEM image of magnetite/maghemite nanoparticles (Figure S1), and TEM image and UV−vis spectrum of 15 nm gold particles (Figure S2). This material is available free of charge via the Internet at http://pubs.acs.org.

CM0603001